

Long-pulse quasi-CW laser cutting of metals

Adrian H. A. Lutey¹  · Alessandro Ascari² · Alessandro Fortunato² · Luca Romoli¹

Received: 17 March 2017 / Accepted: 2 August 2017
© Springer-Verlag London Ltd. 2017

Abstract Long-pulse quasi-CW laser cutting of metals is well suited to small-scale manufacturing settings where process flexibility is of high value and investment capacity is limited. This process refers to cutting operations performed with millisecond laser pulses obtained through modulation of the pump source to achieve continuous-wave (CW) operation over limited time intervals. The ability to minimize heat conduction losses, comprising the vast majority of absorbed laser power at low velocity, allows processing of relatively thick sections compared to what would be possible at the same average power with a CW laser source. The present study quantifies the reduction in heat conduction losses with pulsed exposure by employing a simple power-balance representation of the heat flow problem. Laser-cutting experiments are performed with inert and active assist gases on 1- and 4-mm thick steel samples, varying peak power (0.3–3 kW), pulse energy (0.3–12 J), repetition rate (25–1000 Hz), and velocity (1–40 mm/s). The lowest minimum laser cutting power and highest cutting efficiency are achieved with maximum peak power and lowest permissible pulse overlap for a continuous cut. Under these conditions, heat conduction losses are reduced by more than 60% with nitrogen assist gas compared to CW exposure and more than 50% with oxygen. The calculated average cutting front temperatures are 450–630 °C and

620–900 °C, respectively, well below the melting temperature of steel. Lowest dross adhesion and cut edge surface roughness are obtained with oxygen assist gas, leading to both the lowest minimum average cutting power and highest cut quality. These results demonstrate an efficient process that improves the feasibility of low velocity laser cutting and therefore the range of industrial applications in which laser technology can be employed.

Keywords Laser cutting · Quasi-CW · Millisecond pulses · Thermal modeling · Process efficiency

1 Introduction

Laser cutting of metals has been exploited in manufacturing since shortly after demonstration of the first laser in 1960 [1–4]. This process currently accounts for a large proportion of industrial laser applications, together with laser welding, drilling, surface heat treatment, cleaning, marking, and additive manufacturing [5–7]. The CO₂ laser came to dominate laser cutting for decades due to its high output power and relatively high efficiency compared to solid-state lasers, despite limited optical absorption in metals at the emission wavelength of 10.6 μm. Recently, however, high power fiber lasers have transformed the market due to their much higher wall-plug efficiency, excellent beam quality and emission wavelength of 1064 nm, achieving smaller spot sizes and improved optical absorption in metals [8–10]. Adoption of continuous-wave (CW) and pulsed fiber lasers has been swift across a diverse range of applications from laser cutting and welding of thick metal sections [11, 12] to high-speed processing of thin films [13, 14].

Laser cutting of sheet metal is usually performed with a continuous-wave (CW) laser source in the presence of

✉ Adrian H. A. Lutey
adrian.lutey@unipr.it

¹ Dipartimento di Ingegneria e Architettura, Università degli Studi di Parma, Parco Area delle Scienze, 181/A, Parma, Italy

² Dipartimento di Ingegneria Industriale, Università di Bologna, viale Risorgimento, 2, Bologna, Italy

high pressure coaxial assist gas, expelling material as it is continuously heated and melted by the laser beam. Inherent limits exist in CW laser cutting relating to the stationary heat conduction problem, which has received thorough analytical treatment in the literature [15–19]. It has been demonstrated that heat conduction losses during CW laser cutting can be approximated by a power function of the Peclet number [15]. At low cutting speeds, such losses make up the vast majority of total absorbed laser power necessary to achieve continuous heating and melting of the cutting front. This proportion decreases with increasing cutting speed, leading to more efficient utilization of the incident laser energy and a narrower heat affected zone (HAZ). A consequence of this system behavior is that low-power CW laser sources are disadvantaged in terms of process efficiency by their more limited ability to cut at high speed. This has restricted uptake of laser technology in applications where throughput does not justify the expense of high-power CW laser sources, and component thickness is excessive for ablation with low-power short pulse laser sources. Examples include sizing of 1–5 mm sheet metal in small-scale manufacturing settings and integration of laser cutting into small-scale machining centers.

Pulsed laser materials processing exploits rapid deposition of laser energy to achieve a wide variety of material transformations, from cutting to surface functionalization, while limiting heat conduction losses and formation of the HAZ compared to CW exposure. Laser pulses are generally classified as long (0.1–50 ms), short (1–200 ns) and ultra-short (≤ 10 ps), with equipment costs increasing rapidly as pulse duration decreases. Long-pulse quasi-CW laser irradiation, more typically employed for drilling [20–22], represents a low-cost option that reduces heat conduction losses during low-speed laser cutting and therefore improves process efficiency. Quasi-CW refers to laser pulses obtained through modulation of the pump source to achieve CW operation over limited time intervals. Integration into small-scale machining centers has seen some recent uptake due to the improved process flexibility provided by laser technology (Fig. 1). Processing of components in this setting may require the presence of complex shapes, blind holes or profiles with sharp edges. Machining of these parts cannot be



Fig. 1 Integration of a millisecond pulsed quasi-CW laser source directly into a standard CNC lathe. Photographs courtesy of M.T. S.r.l

performed with traditional turning or milling operations as minimum tool dimensions are in the order of one millimeter. The minimum necessary thickness of material between adjacent cuts can also be drastically reduced with laser processing as there are no cutting forces transmitted to the workpiece, but simply limited thermal effects such as melting and vaporization on a similar scale to the focused beam diameter.

The minimum required average laser power with millisecond pulses is a function of peak power, repetition rate, pulse energy, and velocity. At a given average laser power, the use of high peak power and low repetition rate leads to rapid heating and melting of the kerf volume followed by a relatively long cooling period. Maximum pulse energy is limited by the peak power and lowest repetition rate at which pulse overlap can be maintained for cut continuity. The use of low peak power and high repetition rate, on the other hand, leads to a more constant temperature distribution approaching that of CW laser cutting. The present work quantifies gains achieved in laser cutting efficiency with millisecond pulses compared to CW exposure as a function of the selected laser parameters in terms of minimum average cutting power and volumetric cutting energy. A simple power-balance representation of the heat flow problem is employed to calculate average temperatures at the cutting front, together with the percentage reduction in heat conduction power losses compared to CW exposure under the same conditions. Cut quality is then assessed in terms of edge surface roughness for representative cases where maximum cutting efficiency is achieved.

2 Theory

A simple power-balance representation can be used to define the heat flow problem during CW laser cutting of metals. In this approach, minimum laser power (P_{min}) is expressed as a function of the power required to heat (P_h) and melt (P_m) the cut kerf volume, that lost to thermal conduction (P_l) and the workpiece optical absorptivity at the laser emission wavelength (A) [23]:

$$P_{min} = \frac{P_h + P_m + P_l}{A} \quad (1)$$

where:

$$P_h = \rho C_p (T_m - T_a) v t d \quad (2)$$

$$P_m = \rho H_m v t d \quad (3)$$

where ρ is the material density, C_p the specific heat capacity at constant pressure, H_m the enthalpy of fusion, T_m the melting temperature, T_a the ambient temperature, v the cutting velocity, t the thickness, and d the cut kerf width. Schulz et al. resolved the two-dimensional heat conduction problem

Table 1 Characteristics of the laser setup

| | |
|---|----------|
| Wavelength (<i>nm</i>) | 1064 |
| Pulse Duration (<i>ms</i>) | 0.1 – 50 |
| Repetition Rate (<i>Hz</i>) | 1 – 1000 |
| Beam Quality (BPP, <i>mm · mrad</i>) | 1.6 |
| Focused spot diameter (μm) | 75 |
| Max. average power (<i>W</i>) | 300 |
| Max. pulse energy (<i>J</i>) | 30 |

for CW laser cutting in closed form, finding that P_l could be closely represented by a power function of the Peclet number [15]:

$$P_l = \rho C_p (T_m - T_a) v t d \left(\frac{Pe}{2} \right)^{-0.7} \quad (4)$$

where $Pe = \frac{vd}{2k}$ is the Peclet number and k is the thermal diffusivity. This simplified approach assumes a cylindrical laser source, negligible release of thermal and latent heat from resolidification, negligible radiant and convective heat losses, and negligible influence of the cut kerf and workpiece thickness on the resulting two-dimensional temperature distribution. For the purposes of approximating efficiency gains with long-pulse quasi-CW laser irradiation, however, this representation lends itself to modification by replacing T_m in Eq. 4 with the average cutting front temperature, T_{av} . At minimum cutting power, the average cutting front temperature should be lower than T_m under pulsed conditions, owing to the transient nature of heating and melting. Equations 2 and 3 remain unchanged as the power required to continuously heat and melt the kerf volume is constant regardless of the exposure type. This approach allows relatively straight-forward calculation of T_{av} from experimental results and approximation of the reduction in P_l compared to CW laser cutting.

3 Experimental

3.1 Test samples

36NiCrMo4 (AISI 9840) steel samples of thickness 1 and 4 mm were utilized for laser-cutting experiments. These two thicknesses were chosen as representing thin and thick workpieces relative to the available laser power, respectively, allowing investigation into the effects of long-pulse quasi-CW laser irradiation across the widest possible process parameter range. This particular steel was chosen due to its widespread use in structural and engineering applications, having good mechanical strength, hardenability and toughness at relatively low cost.

3.2 Laser source

A 300 W average power IPG YLR-300/3000-QCW-MM-AC-Y14 millisecond pulsed quasi-CW fiber laser source equipped with an II-VI FiberLight laser-cutting head was utilized for all experiments. The cutting head was mounted with a 1 mm diameter nozzle and a 90 mm focal length focusing lens with adjustable focus. The maximum attainable peak power was 3 kW, with a maximum pulse energy of 30 J. The laser could also emit in CW with an output power of 300 W. Characteristics of the laser setup are given in Table 1.

3.3 Procedure

The laser-cutting head was positioned with a nozzle stand-off distance of 0.5 mm from the workpiece surface. Laser focus was set at 0.5 mm below the surface for 1 mm samples and 2 mm below the surface for 4 mm samples, resulting in a spot diameter of 75 μm at the center of each section and approximately 100 and 200 μm , respectively, at the surface. Tests were performed with nitrogen and oxygen assist gases at pressures of 500 and 300 kPa, respectively. Ten different

Table 2 Laser parameter groups utilized for tests performed on 1 mm thick samples

| Parameter Group | 1 | 2 | 3 | 4 | 5 | 6 | 7 | 8 | 9 | 10 |
|---------------------------------|------|-----|-----|-----|-----|-----|-----|-----|-----|-----|
| Exposure type* | P | P | P | P | P | P | CW | P | P | P |
| Peak power (<i>kW</i>) | 3 | 3 | 3 | 3 | 2 | 1 | 0.3 | 3 | 3 | 3 |
| Repetition rate (<i>Hz</i>) | 1000 | 500 | 333 | 250 | 500 | 500 | – | 500 | 500 | 500 |
| Pulse duration (<i>ms</i>) | 0.1 | 0.2 | 0.3 | 0.4 | 0.3 | 0.6 | – | 0.2 | 0.2 | 0.2 |
| Max. pulse energy (<i>J</i>) | 0.3 | 0.6 | 0.9 | 1.2 | 0.6 | 0.6 | – | 0.6 | 0.6 | 0.6 |
| Max. average power (<i>W</i>) | 300 | 300 | 300 | 300 | 300 | 300 | 300 | 300 | 300 | 300 |
| Velocity (<i>mm/s</i>) | 20 | 20 | 20 | 20 | 20 | 20 | 20 | 10 | 30 | 40 |
| Pulse overlap (%) | 73 | 47 | 20 | 0 | 47 | 47 | – | 73 | 20 | 0 |

*P pulsed, CW continuous wave

Table 3 Laser parameter groups utilized for tests performed on 4 mm thick samples

| Parameter Group | 1 | 2 | 3 | 4 | 5 | 6 | 7 | 8 | 9 | 10 |
|---------------------------------|------|-----|-----|-----|-----|-----|-----|-----|-----|-----|
| Exposure type* | P | P | P | P | P | P | CW | P | P | P |
| Peak power (<i>kW</i>) | 3 | 3 | 3 | 3 | 2 | 1 | 0.3 | 3 | 3 | 3 |
| Repetition rate (<i>Hz</i>) | 1000 | 100 | 50 | 25 | 50 | 50 | – | 50 | 50 | 50 |
| Pulse duration (<i>ms</i>) | 0.1 | 1 | 2 | 4 | 3 | 6 | – | 2 | 2 | 2 |
| Max. pulse energy (<i>J</i>) | 0.3 | 3 | 6 | 12 | 6 | 6 | – | 6 | 6 | 6 |
| Max. average power (<i>W</i>) | 300 | 300 | 300 | 300 | 300 | 300 | 300 | 300 | 300 | 300 |
| Velocity (<i>mm/s</i>) | 2 | 2 | 2 | 2 | 2 | 2 | 2 | 1 | 3 | 4 |
| Pulse overlap (%) | 97 | 73 | 47 | 0 | 47 | 47 | – | 73 | 20 | 0 |

*P pulsed, CW continuous wave

laser parameter groups were utilized for each sample thickness and assist gas type, systematically varying repetition rate, pulse energy, peak power and velocity over as wide a range as possible. The details of all parameter groups are given in Tables 2 and 3 for 1 and 4 mm samples, respectively. In all cases, groups 1 to 4 saw variation of pulse repetition rate from 1000 Hz to a minimum value at which the pulse overlap approached 0%. Peak power was held constant, with pulse duration and pulse energy increased to maintain a maximum average power of 300 W. Groups 5 to 7 instead saw variation of peak power down to a minimum value of 300 W with constant repetition rate, pulse energy and pulse overlap. Pulse duration was increased to maintain a maximum average power of 300 W up to the limiting case of 100% duty cycle with CW exposure in group 7. Groups 8 to 10 saw variation of exposure velocity with constant laser parameters. Lower repetition rates and therefore higher pulse energies were utilized for the 4 mm samples due to lower attainable cutting velocities and therefore higher pulse overlap.

Within each test group, individual laser exposures were performed over a length of 40 mm, starting from outside the specimen. Laser power was varied from 100 to 10% at intervals of 10%, with two repetitions performed on different samples for each parameter group. Minimum cutting power was defined as the power at which complete uninterrupted material penetration was achieved for the entire 40 mm cut length. Volumetric cut energy was taken as the minimum

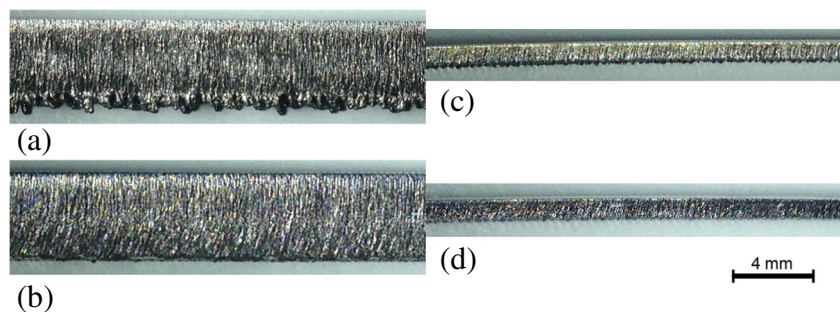
cutting power divided by the kerf removal rate. The resulting cut edges obtained at maximum cutting efficiency were analyzed with a Taylor Hobson Talysurf CCI optical profiler with 50× objective. Profile measurements were performed at the center of the cut section for 1 mm samples and at 2.6 mm from the surface for 4 mm samples (2/3 depth), over a length of 4.17 mm in both cases. Due to the relatively limited field of view of the optical profiler (340 × 340 μm), data stitching was performed to achieve the required length.

4 Results and discussion

Laser cutting was successfully performed with all parameter groups excluding 4 and 10 for 1 mm samples, where pulse overlap was insufficient, and 7 for 4 mm samples, where laser power was insufficient. Photographs of the resulting cut edges achieved with the lowest minimum average cutting power across all test groups are presented in Fig. 2. The cut edges are consistent in form across the entire length and generally of good quality; however, some dross is evident on the 4 mm sample with nitrogen assist gas.

Minimum average cutting power and volumetric cutting energy for the 1 mm samples are presented in Fig. 3 for all test parameter groups. The main varied parameter in each case is displayed above the upper horizontal axis. Parameter group 7 provides reference values for CW cutting at 20 mm/s with nitrogen and oxygen assist gas, 210 and

Fig. 2 Photographs of laser cut edges achieved with minimum average power: **a** 4 mm thickness, parameter group 4, nitrogen assist gas, **b** 4 mm thickness, parameter group 4, oxygen assist gas, **c** 1 mm thickness, parameter group 3, nitrogen assist gas, and **d** 1 mm thickness, parameter group 3, oxygen assist gas



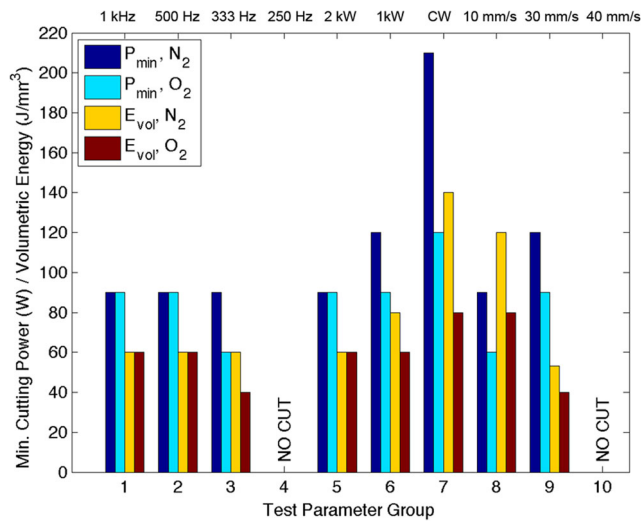


Fig. 3 Minimum average laser-cutting power (P_{min}) and volumetric cutting energy (E_{vol}) for 1 mm samples

120 W, respectively. Cutting with oxygen required approximately 40% less laser power due to additional energy provided by the exothermic oxidation of iron [24]. In comparison, long-pulse quasi-CW laser cutting at a repetition rate of 1000 Hz (group 1) required 90 W with both nitrogen and oxygen. By reducing the repetition rate to 333 Hz (group 3), minimum average cutting power dropped to 60 W for oxygen but remained constant at 90 W for nitrogen. These conditions represent the lowest achievable minimum cutting power at 20 mm/s, a reduction of 40–50% compared to CW exposure. At 250 Hz (group 4), pulse overlap was insufficient to achieve a complete cut, resulting in discontinuous perforation of the samples. By reducing peak laser power to 1 kW (group 6) and then 300 W (CW conditions in group 7), minimum average cutting power increased significantly. Volumetric cutting energy increased at 10 mm/s

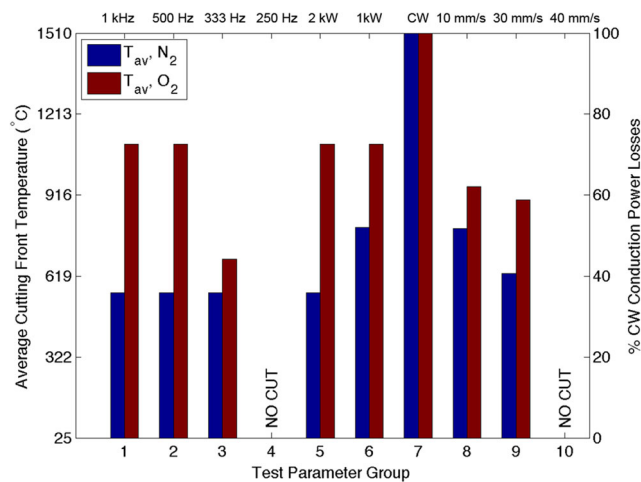


Fig. 4 Calculated average cutting front temperature (T_{av}) and percentage of CW thermal conduction power losses for 1 mm samples

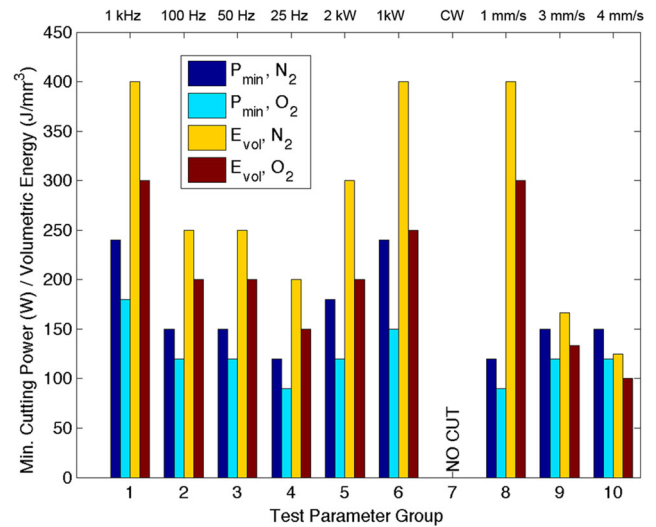


Fig. 5 Minimum average laser-cutting power (P_{min}) and volumetric cutting energy (E_{vol}) for 4 mm samples

(group 8) and decreased at 30 mm/s (group 9) compared to exposure at 20 mm/s with the same laser parameters (group 2). This effect is due to decreasing power conduction losses with increasing velocity. At 40 mm/s (group 10), pulse overlap was insufficient to achieve a continuous cut.

Average cutting front temperatures are presented in Fig. 4, calculated by substituting the experimental minimum average cutting power into Eq. 1. Equivalent absorption, A , was 0.5 with nitrogen assist gas and 0.88 with oxygen. Reaction power made up approximately 45% of the absorbed power in the latter case [4]. These values led to a calculated kerf temperature equal to the melting temperature (1510 °C) under CW conditions with parameter group 7. Calculated average cutting temperatures were generally higher with oxygen due to additional energy provided by the

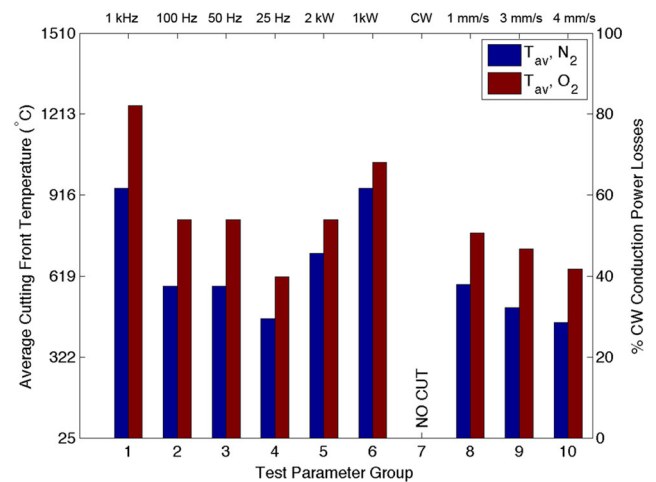


Fig. 6 Calculated average cutting front temperature (T_{av}) and percentage of CW thermal conduction power losses for 4 mm samples

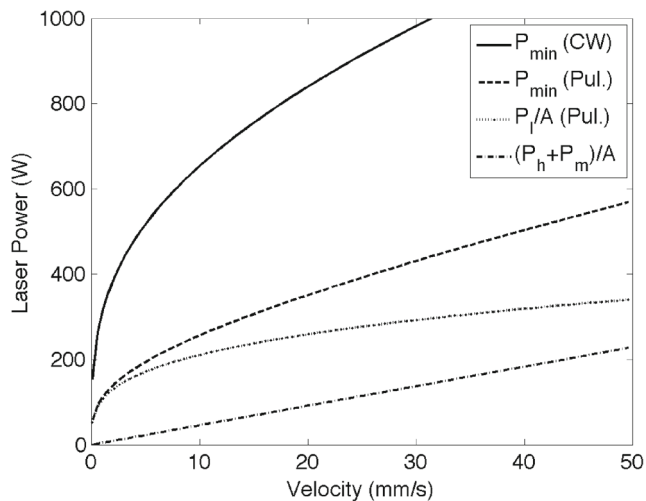


Fig. 7 Calculated minimum laser power, P_{min} , for CW and long-pulse quasi-CW (0–20% overlap) cutting of 4 mm thick steel with nitrogen assist gas, together with P_l/A and $(P_h + P_m)/A$ for long pulses

oxidation reaction. Nonetheless, significant reductions in conduction power losses were observed in both cases, with P_l as low as 36% of the CW value with nitrogen and 44% with oxygen. As with the minimum average cutting power, T_{av} decreased with decreasing repetition rate and increased with decreasing peak power.

The effect of process parameter choice was more evident at lower cutting speeds with thicker samples due to the wider range of conditions (Figs. 5 and 6). CW laser cutting of 4 mm thick steel at 2 mm/s was not possible with an average power of 300 W; however, long-pulse quasi-CW laser cutting at a repetition rate of 1000 Hz (group 1) required 240 and 180 W average power with nitrogen

and oxygen assist gases, respectively. A reduction in repetition rate from 1000 to 25 Hz (groups 1 to 4) saw a large reduction in minimum cutting power to 120 and 90 W for nitrogen and oxygen, respectively, at the lowest repetition rate. The calculated average temperature fell from 941 and 1244 °C at 1000 Hz to 464 and 617 °C at 25 Hz. The percentage reduction in P_l is very similar to the reduction in P_{min} in this case due to the exceedingly high value of P_l at low velocities compared to P_h and P_m , which take on values of 3.3 W and 1.3 W according to Eqs. 2 and 3, respectively. Despite low pulse overlap with group 4, a continuous cut was achieved for 4 mm thick samples. As with the 1 mm samples, the lowest repetition rate at which a full cut could be achieved yielded the lowest minimum cutting power. Similarly, minimum average cutting power and T_{av} increased with decreasing peak power, to the point where a full cut was not achieved at maximum laser power under CW conditions (group 7). Large decreases in volumetric cutting energy with increasing velocity were observed over the velocity range 1–4 mm/s (groups 8 to 10), while this parameter was generally much higher for 4 mm than for 1 mm samples due to the much lower velocities involved in the former case. This result confirms a decrease in the proportion of laser power lost to conduction with increasing velocity.

Despite the largely different process parameters employed for 1 and 4 mm thick samples, the calculated heat conduction losses and average cutting temperatures are minimum, within the ranges 30–40% of CW exposure and 450–630 °C, respectively, for tests performed with low pulse overlap (0–20%) and nitrogen assist gas. Heat conduction losses are therefore minimized where complete penetration of the workpiece is achieved in as few laser pulses as possible. The calculated heat conduction

Fig. 8 Measured cut edge profile of 1 mm samples subject to parameter group 3 with **a** nitrogen and **b** oxygen assist gas

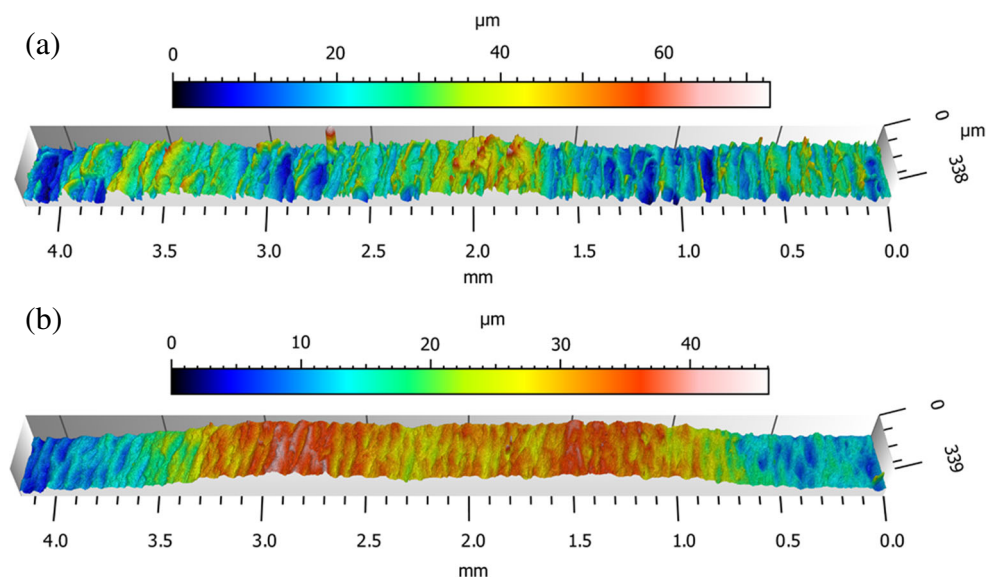
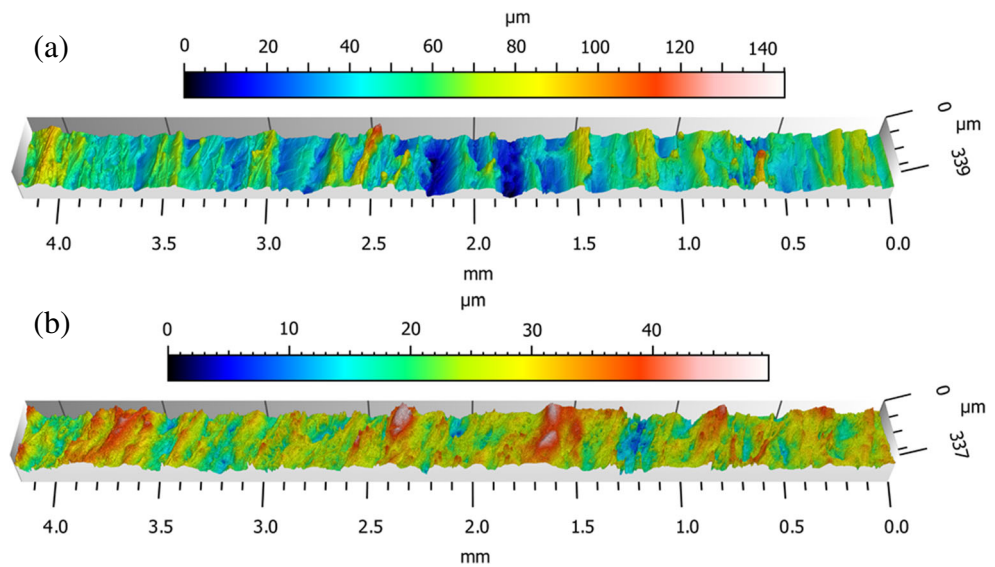


Fig. 9 Measured cut edge profile of 4 mm samples subject to parameter group 4 with **a** nitrogen and **b** oxygen assist gas



losses compared to CW exposure and average cutting front temperatures are instead within the ranges 40–60% and 620–900 °C for tests performed with low pulse overlap (0–20%) and oxygen assist gas. The higher average temperature results in less difference between CW and long-pulse quasi-CW cutting in terms of minimum cutting power.

Figure 7 presents the calculated minimum cutting power as a function of velocity for 4 mm samples with nitrogen assist gas for CW exposure and for long pulses with minimum overlap. P_l/A and $(P_h + P_m)/A$, whose sum is P_{min} , are also presented for pulsed exposure. Long-pulse quasi-CW exposure can be seen to reduce the difference between the laser power contributing to the cutting process and that lost to heat conduction, with the former increasing in proportion at higher velocities.

Cut section profiles are presented in Figs. 8 and 9 for 1 and 4 mm samples produced with parameter groups 3 and 4, respectively. Measured cut edges corresponded to 10% higher laser power than the minimum value so as to reflect realistic industrial cutting conditions. Values of S_a and S_q over the 4.17×0.34 mm sample area are provided in Table 4 for all measurements. Use of nitrogen and oxygen assist gases presents little difference in terms of roughness for the

1 mm samples; however, considerably lower surface roughness was observed with oxygen for the 4 mm samples. This effect, contrary to what is typically observed during CW laser-cutting, may be due to the more continuous nature of energy provided to the kerf volume with the addition of reaction power from oxidation, which is expected to follow a more gradual temporal profile than the laser pulse. Cutting with inert gas and very low pulse overlap, on the other hand, leads to strong variation in instantaneous energy delivered along the cut edge. These results have important implications for industrial application of long-pulse quasi-CW laser cutting, as use of oxygen assist gas leads to both lower minimum laser power and cut edge roughness for thick specimens.

5 Conclusion

Though it is clear that the applicability of long-pulse quasi-CW laser sources for metal cutting is likely to be limited to low throughput manufacturing settings for the time being, many opportunities exist within small and medium sized enterprises where laser technology could provide greater process flexibility than conventional manufacturing techniques. It has been shown within the present work that millisecond laser pulses can significantly reduce the minimum required laser-cutting power at low velocities, permitting thicker components to be processed than would be possible with CW exposure. For the full benefit of this technology to be exploited, it is important that laser exposure is performed with the highest possible peak power and lowest permissible pulse overlap for a continuous cut, achieving complete penetration of the workpiece in as few laser pulses as possible. Under these conditions, highest cutting

Table 4 Measured surface roughness for 1 mm and 4 mm samples produced with parameter groups 3 and 4, respectively

| Sample | S_a (μm) | S_q (μm) |
|-----------------------|-------------------------|-------------------------|
| 1 mm, N_2 , Group 3 | 7.64 | 9.59 |
| 1 mm, O_2 , Group 3 | 8.48 | 9.49 |
| 4 mm, N_2 , Group 4 | 13.2 | 16.7 |
| 4 mm, O_2 , Group 4 | 4.91 | 6.27 |

efficiency is achieved and the potential to increase removal rates is improved. Heat conduction losses, making up the vast majority of absorbed laser power at low velocity, can be reduced by more than 60% compared to CW exposure with nitrogen assist gas and more than 50% with oxygen assist gas. Reductions of this type are possible due to lower average cutting front temperatures, in the order of 450–630 °C with nitrogen assist gas and 620–900 °C with oxygen, significantly less than the melting temperature of steel. Cut edge surface roughness and dross adhesion are lowest with oxygen assist gas, leading to the optimum scenario of lowest minimum average cutting power and highest cut quality. In light of these results, long-pulse quasi-CW laser technology represents a potential candidate for material processing in many small-scale industrial settings.

Acknowledgements The authors would kindly like to thank M.T. S.r.l., specifically Gianluca Marchetti, Michael Dina and Paolo Leonardi (Studio Genius), for technical and financial support throughout the duration of this project. The authors would also like to thank Andrea Moselli for his help in performing and analyzing test samples.

References

- Lunau F, Paine E, Richardson M, Wijetunge M (1969) High-power laser cutting using a gas jet. *Opt Technol* 1(5):255–258
- Babenko V, Tychinskii V (1973) Gas-jet laser cutting (Review). *Sov J Quantum Electron* 2(5):399–410
- von Allmen M (1987) *Laser-beam interactions with materials*. Springer, Berlin
- Ready J, Farson D, Feeley T (eds) (2001) *LIA Handbook of laser materials processing*. Springer, Berlin
- Kannatey-Asibu E (2009) *Principles of laser materials processing*. Wiley, Hoboken
- Gu D, Meiners W, Wissenbach K, Poprawe R (2012) Laser additive manufacturing of metallic components: materials, processes and mechanisms. *Int Mater Rev* 57(3):133–164
- Frazier W (2014) Metal additive manufacturing: a review. *J Mater Eng Perform* 23(6):1917–1928
- Gabzdyl J (2008) Materials processing: fibre lasers make their mark. *Nat Photonics* 2(1):21–23
- Mahrle A, Beyer E (2009) Theoretical aspects of fibre laser cutting. *J Phys D Appl Phys* 42(17):175,507
- Powell J, Al-Mashikhi S, Kaplan A, Voisey K (2011) Fibre laser cutting of thin section mild steel: an explanation of the ‘striation free’ effect. *Opt Lasers Eng* 49(8):1069–1075
- Li S, Chen G, Katayama S, Zhang Y (2014) Relationship between spatter formation and dynamic molten pool during high-power deep-penetration laser welding. *Appl Surf Sci* 303:481–488
- You D, Gao X, Katayama S (2014) Monitoring of high-power laser welding using high-speed photographing and image processing. *Mech Syst Signal Process* 49(1-2):39–52
- Coelho J, Abreu M, Pires M (2000) High-speed laser welding of plastic films. *Opt Lasers Eng* 34(4):385–395
- Lee D, Patwa R, Herfurth H, Mazumder J (2013) High speed remote laser cutting of electrodes for lithium-ion batteries: anode. *J Power Sources* 240:368–380
- Schulz W, Becker D, Franke J, Kemmerling R, Herziger G (1993) Heat conduction losses in laser cutting of metals. *J Phys D Appl Phys* 26(9):1357–1363
- Kaplan A (1996) An analytical model of metal cutting with a laser beam. *J Appl Phys* 79(5):2198–2208
- Schulz W, Kostykin V, Nießen M, Michel J, Petring D, Kreutz E, Poprawe R (1999) Dynamics of ripple formation and melt flow in laser beam cutting. *J Phys D Appl Phys* 32(11):1219–1228
- Duan J, Man H, Yue T (2001) Modelling the laser fusion cutting process: I. Mathematical modelling of the cut kerf geometry for laser fusion cutting of thick metal. *J Phys D Appl Phys* 34(14):2127–2134
- Scintilla L, Tricarico L, Wetzig A, Beyer E (2013) Investigation on disk and CO_2 laser beam fusion cutting differences based on power balance equation. *Int J Mach Tools Manuf* 69:30–37
- Yilbas B (1997) Parametric study to improve laser hole drilling process. *J Mater Process Technol* 70(1-3):264–273
- Hanon M, Akman E, Genc Oztoprak B, Gunes M, Taha Z, Hajim K, Kacar E, Gundogdu O, Demir A (2012) Experimental and theoretical investigation of the drilling of alumina ceramic Nd: YAG pulsed laser. *Opt Laser Technol* 44(4):913–922
- Zhang Y, Shen Z, Ni X (2014) Modeling and simulation on long pulse laser drilling processing. *Int J Heat Mass Transfer* 73:429–437
- Jiang H, Woodard P (2005) Methodology of generic modeling as applied to energy coupling of CO_2 laser material interaction. *Opt Lasers Eng* 43(1):19–31
- Powell J, Petring D, Kumar R, Al-Mashikhi S, Kaplan A, Voisey K (2009) Laser-oxygen cutting of mild steel: the thermodynamics of the oxidation reaction. *J Phys D Appl Phys* 42(1):015,504